Effect of Axial Substitution on the Optical Limiting Properties of Indium Phthalocyanines

James S. Shirk,*,† Richard G. S. Pong,† Steven R. Flom,† Heino Heckmann,‡ and Michael Hanack*,‡

Optical Sciences Division, Naval Research Laboratory, Washington, D.C. 20375, and the Institut für Organische Chemie, Lehrstuhl für Organische Chemie II, Auf der Morgenstelle 18, Universität Tübingen, D-72076 Tübingen, Germany

Received: September 14, 1999; In Final Form: December 6, 1999

Nonlinear absorption, refraction, and optical limiting by a series of monoaxially chloro- and aryl-substituted indium(III) phthalocyanines are described. The absorption cross sections and temporal evolution of the low-lying excited states are also reported. A large nonlinear absorption that increased with wavelength between 500 and 590 nm was observed in each material. The nanosecond nonlinear absorption and the optical limiting are shown to be dominated by a strong excited state absorption from an orientationally averaged triplet state. We derive and experimentally confirm the relation between the molecular absorption cross sections and the fluence-dependent nonlinear absorption coefficients. The effective nonlinear refraction on the nanosecond time scale was reduced because the electronic contribution to the nonlinear refractive index was of the opposite sign from the thermal contribution. An optical limiter using the new material, *p*-(trifluoromethyl)phenylindium(III) tetra-*tert*-butylphthalocyanine [(*t*-Bu)$_4$PcIn(*p*-TMP)], showed a much lower threshold for optical limiting and a much lower transmission at high fluences than previously reported indium phthalocyanine limiters. This improved optical limiting was due both to the larger nonlinear absorption coefficient and to the design of the limiter device. The optical properties of the In phthalocyanine moiety were found to be surprisingly robust to structural changes in the axial position.

Introduction

Devices that can control the amplitude, phase, polarization, or direction of optical beams have a variety of important applications. Since the lack of appropriate nonlinear materials has been a primary barrier to the development of such devices, there has been a continuing interest in the development of new nonlinear optical materials. Some of the more recent organic nonlinear materials[1−4] have shown considerable promise for optical limiting. This paper describes the optical properties of a new set of materials designed for optical limiting applications.

Optical limiters have a transmission that varies with the incident intensity. The transmission is high at normal light intensities and low for intense beams. Ideally, this intensity-dependent transmission can limit the transmitted light intensity so that it is always below some maximum value, hence the name. Among the functions such devices can perform, one of the most useful is protecting optical elements and sensors against damage by exposure to sudden high-intensity light. For such applications all-optical devices are preferred over mechanical or electrooptical devices since they can provide the fast response speeds that are required. Thus, the better optical limiters usually rely on a third-order or pseudo-third-order response, such as nonlinear absorption or refraction. Nonlinear absorption, where the material's absorbance increases with the intensity of the incident light, is obviously useful for this application.

One mechanism that has been especially effective at producing large nonlinear absorption is a sequential two-photon absorption. A simple energy level diagram where this process can occur is shown in Figure 1. If the material has an excited state absorption cross section, σ_{ex}, larger than the ground state cross section, σ_0, and, if the incident light is sufficiently intense so that a significant population accumulates in the excited state, the effective absorption coefficient of the material increases. To achieve the largest nonlinear absorption, both a large excited state absorption cross section and a long excited state lifetime are required. When the lifetime of the excited state being pumped is longer than the pulse width of the incident light, the changes in the absorbance and the refractive index are fluence (J/cm^2), not intensity (W/cm^2), dependent.[5] Thus, in materials with long upper state lifetimes, it is the fluence rather than the intensity that is limited. Limiting the fluence is usually desirable, since damage to optical devices is also often fluence dependent. This sequential two-photon absorption process has also been called reverse saturable absorption or excited state absorption.[1,4,6,7]

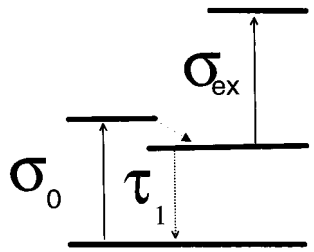

Figure 1. Lowest energy levels of a simple nonlinear absorber.

Some criteria necessary for a large, positive nonlinear absorption are apparent. These include a large excited state cross section, σ_{ex}, and a large difference between the ground and excited state absorption cross sections ($\sigma_{ex} - \sigma_0$). A variety of

† Code 5613, Optical Sciences Division, Naval Research Laboratory, Washington, DC.

‡ Institut für Organische Chemie der Eberhard-Karls Universität Tübingen.

10.1021/jp993254j
Published on Web 02/01/2000

SCHEME 1

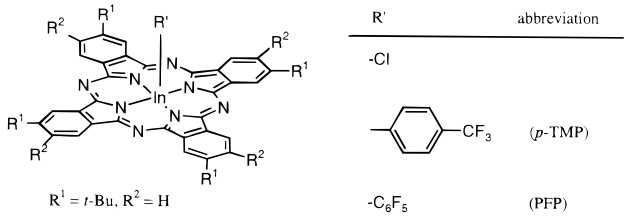

organic and organometallic materials have been found to fulfill these conditions. Materials known to possess a positive nonlinear absorption in the visible include phthalocyanines,[1,8−12] porphyrins,[7,13−15] organometallic cluster compounds,[16−21] and other materials.[22−31]

The condition that σ_{ex} is greater than σ_0 is necessary but it is *not sufficient* for a useful optical limiter material. A practical optical limiter must operate over the wide range of incident intensities that might be encountered. The nonlinear response should possess a low threshold and remain large over a large range of fluences before the nonlinearity saturates. A high saturation fluence normally requires a high concentration of the material in the optical beam. This, in turn, requires a highly soluble compound, a pure liquid, or a solid film that can be prepared with good optical quality. Many of the dyes used as nonlinear absorbers tend to aggregate at high concentration. Intermolecular interactions are usually deleterious, so extensive aggregation needs to be suppressed. In addition, the material must possess a high linear transmission and a large nonlinear absorption over a broad spectral bandwidth as well as a high threshold for damage. Furthermore, the nonlinear absorption must appear with a subnanosecond response time. Meeting all these criteria is a significant chemical challenge. Among the large number of nonlinear absorbers that have been identified, the lead phthalocyanine, tetrakis(β-cumylphenoxy)-PbPc,[9,32] the indium phthalocyanine, (*t*-Bu)4InPcCl,[33] and some substituted porphyrins[7,13] have been used to construct optical limiters that approached the characteristics necessary for a practical device.

One strategy for the development of improved optical limiters is to modify some of the better materials systematically. To pursue this tactic, we recently described a synthetic technique to vary the axial substituent of indium phthalocyanines.[34] Variations in axial substitution can (1) alter the electronic structure of the phthalocyanine, (2) introduce a dipole moment perpendicular to the macrocycle, and (3) introduce new steric effects that alter the spatial relationships between neighboring molecules thus altering the magnitude of the intermolecular interactions.

The present paper presents a study of the optical properties of a series of monoaxially substituted chloro- and arylindium(III) phthalocyanines R_xInPc(R′) shown in Scheme 1. The purpose is to study the effect of some new axial substituents on the nonlinear optical properties of the indium phthalocyanines. The materials studied in most detail were those materials with the peripheral substituent R^1 = *tert*-butyl, $x = 4$; and the axial substituent R′ = chloro-, *p*-trifluoromethylphenyl- (*p*-TMP), and perfluorophenyl- (PFP). The latter materials represent the more promising of a larger group of related materials that were synthesized. Compared with the chloro ligand, the larger aryl substituents can alter the packing of the molecules in the solid state and the tendency to aggregate in solution. Controlling aggregation is important because it can alter the excited state relaxation time and the effective nonlinear absorption of the material. Variations in the electron-withdrawing properties of the substituted aryl ligands should lead to variations in the electronic properties including the ground state dipole moment. Each of these effects can influence the NLO properties that are important for limiting.

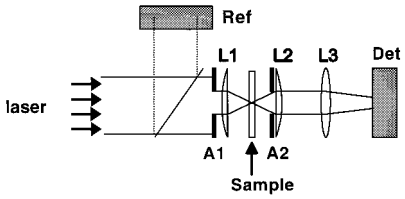

Figure 2. Apparatus for the nanosecond optical limiting and Z-scan experiments. Det and Ref are the signal and reference detectors, respectively. Lens L1 focuses the laser onto the nonlinear sample and L2 recollimates the light. L3 transfers the light to the detector. The apertures A1 and A2 define the *f* number of the focusing and collection optics.

Experimental Apparatus

The nanosecond experiments were performed using the apparatus shown in Figure 2. The input beam was a spatially filtered beam from one of the laser sources described below. The spatial profile of the input beam usually showed a greater than 96% correlation with a Gaussian profile. The laser intensity was controlled by wave plate/polarizer combinations.

The laser source for the wavelength-dependent nanosecond experiments was an optical parametric oscillator (OPO) (Continuum Surelite) pumped by the third harmonic of a Nd:YAG laser. The pulse width was 2.5 ns. Some of the nanosecond experiments at 532 nm used a doubled Nd:YAG laser with an 8 ns pulse width. The experiments at low energies were conducted at 10 Hz. For incident fluences above about 10 mJ/cm^2, the repetition rate was reduced to 0.5 Hz. This removed any effect of persistent thermal effects. For incident fluences above about 50 mJ/cm^2, the experiments were single shots and the sample was translated between the shots to provide a fresh sample for each data point.

Two different sets of focusing optics were used. A Gaussian input beam, focused using approximately *f*/45 optics, was used for nonlinear absorption experiments. The focal spot size, *f*/number, and the beam quality as measured by M^2 were determined from knife edge scans at several positions along the beam path near the focus. The measured M^2 increased from 1.1 at 530 nm to 1.3 at 610 nm. A diffraction limited Gaussian beam would have $M^2 = 1$. The measured focal spot size was within about 10% of that expected for a Gaussian beam between 530 and 610 nm.

In the *f*/5 limiter, the input laser beam was expanded so that only the central 10% was transmitted by the first aperture. This gives the beam an approximately flat top intensity profile. The lens L1 was a corrected multiplet, which focused the light to a spot with a measured beam radius of 2.5 ± 0.1 μm at 532 nm. The expected radius for a diffraction limited *f*/5 Airy distribution is 2.2 μm at 532 nm. With the OPO as a source, the beam radius was measured to be 2.6 ± 0.1 μm at 550 nm.

In both cases, the light passing through the sample was recollimated by L2 and focused by lens L3 onto the detector. With no exit aperture (A2), lens L2 provided approximately *f*/0.8 collection optics. For optical limiting measurements, the exit aperture (A2) was set to the diameter appropriate for an *f*/5 optical system. The sample was mounted on a translation stage and translated through the focus for the Z-scan experiments. For optical limiting and nonlinear transmission measurements, the sample position was adjusted about the focus to give

the smallest transmitted energy for incident energies near the limiting threshold.

The time-resolved experiments included degenerate four-wave mixing (DFWM) studies and spectrally resolved transient absorption (TA). They were performed using a dye laser that is synchronously pumped by the second harmonic of a CW mode-locked Nd:YAG laser. The dye laser output was amplified in a three-stage dye amplifier pumped using the second harmonic of a regenerative Nd:YAG amplifier seeded with the fundamental of the mode-locked Nd:YAG laser. The 10 Hz output of the laser system provided 1.2 ps fwhm pulses with energies up to 1 mJ and was tuned to 589 nm for the DFWM experiments and to 725.5 nm for the transient absorption experiments.

For the transient absorption (TA) experiments, the laser output was split into two beams. The first provided an excitation source. The remaining beam was focused into a cuvette of flowing water to generate a continuum probe pulse. The continuum light was filtered and subsequently split into signal (S) and reference (R) channels. The continuum light in the signal channel was directed through the sample. Both channels were coupled to a $^1/_4$ m monochromator via optical fiber bundles and simultaneously detected by a CCD camera. ΔOD was calculated from the absorbance ($-\log_{10}(S/R)$) of the excited sample less the absorbance of the unexcited sample. Time resolution was obtained by varying the arrival of the excitation pulse relative to that of the continuum pulse. The polarization of the excitation pulse was at 54.7° relative to that of the continuum pulse to eliminate the influence of orientational effects.

DFWM experiments were carried out in the phase conjugate geometry that has been described previously.[35,36] Time resolution was obtained by optically delaying either of the two counter-propagating beams. Two polarization combinations were used in these experiments, the first with all four beams copolarized, called the *xxxx* polarization, and the second with probe and signal beam cross polarized with respect to the two counter-propagating beams, called the *xyyx* polarization.

The ground state absorption spectra were recorded on a Perkin-Elmer Lambda 9 spectrophotometer.

Results

Linear Spectroscopy. The linear spectra of (*t*-Bu)$_4$PcInCl, perfluorophenylindium(III) tetra-*tert*-butylphthalocyanine [(*t*-Bu)$_4$PcInPFP], and *p*-(trifluoromethyl)phenylindium(III) tetra-*tert*-butylphthalocyanine [(*t*-Bu)$_4$PcIn(*p*-TMP)], have been reported.[34] In dilute solution the spectra are characterized by the strong Q-band near 697 nm and the strong B band near 340 nm that are typical of metal phthalocyanines. There is less than a 1 nm shift in the position of the Q-band between these compounds. The region of interest for optical limiting is in the high-transmission region between 420 and 600 nm, between the intense Q and B bands. The nonlinear optical experiments were performed on samples with concentrations between 22 and 45 mM in $CHCl_3$. The spectra of these solutions in the regions important to the NLO experiments are shown in Figure 3. The path lengths were 12−35 μm. At these high concentrations, the absorbance in the regions near the Q- and B-bands are off scale. Also shown in Figure 3 are the spectra of 7 mM solutions with a 200 μm path and 7×10^{-6} M solutions with a 1 cm path. The sample absorbance of the dilute solution was normalized to compare the shape of the bands in the region of interest.

The spectra of the aryl-substituted materials in the region of interest for limiting, 450−620 nm, are shown on an expanded scale in Figure 4. Each of these materials has a high transmission near 500 nm. (*t*-Bu)$_4$PcInCl has an absorption cross section of

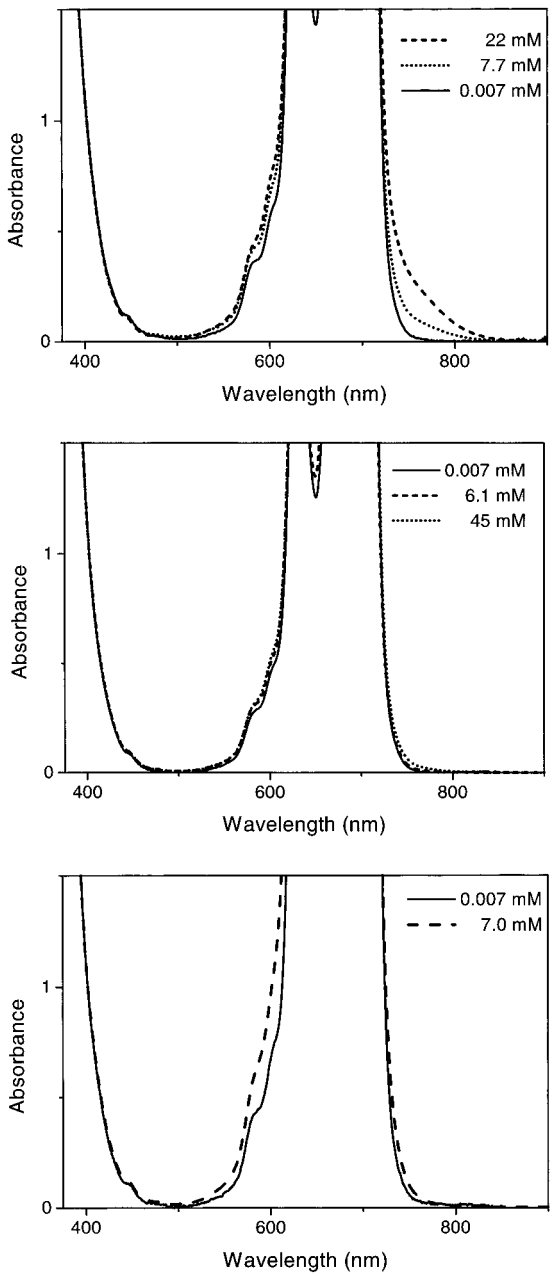

Figure 3. Normalized absorption spectra of (a, top) (*t*-Bu)$_4$PcInCl, (b, middle) (*t*-Bu)$_4$PcIn(*p*-TMP), and (c, bottom) (*t*-Bu)$_4$PcInPFP, at different concentrations in $CHCl_3$.

less than 2×10^{-18} cm^2, corresponding to a molar extinction coefficient of less than 500 L/(mol cm), over the range 460−533 nm, even in concentrated solutions. The measured absorption coefficients of the aryl-substituted materials vary by less than ±30% from that found in (*t*-Bu)$_4$PcInCl over the range 430−610 nm. In the range 500−610 nm where the nonlinear optical studies were performed, (*t*-Bu)$_4$PcInPFP had a systematically larger absorption coefficient and (*t*-Bu)$_4$PcIn(*p*-TMP) had a slightly smaller ground state absorption than the (*t*-Bu)$_4$PcInCl solution.

Aggregation is generally undesirable in a limiter material since strong intermolecular interactions usually add relaxation pathways, shorten the excited state lifetime, and reduce the effective nonlinear absorption. Aggregation in the phthalocyanines usually results in spectral shifts and changes in the band shapes.[37] The observed band shapes in Figure 3 change only a little over a concentration range from about 10^{-5} M to greater than 10 mM in each material. The largest difference in

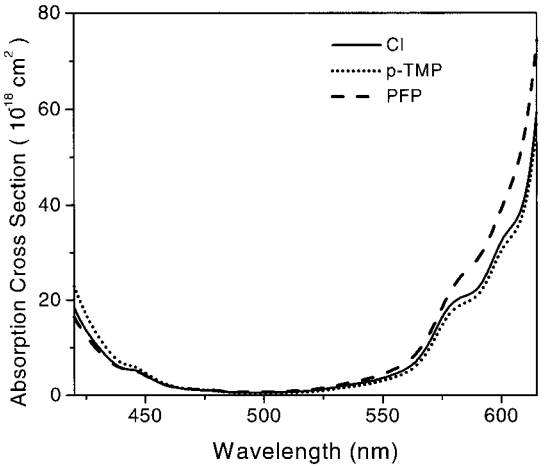

Figure 4. Ground state absorption cross sections for (*t*-Bu)$_4$PcInCl, (*t*-Bu)$_4$PcIn(*p*-TMP), and (*t*-Bu)$_4$PcInPFP in the region where each has a large nonlinear absorption. This is the weakly absorbing region where the materials are useful optical limiters.

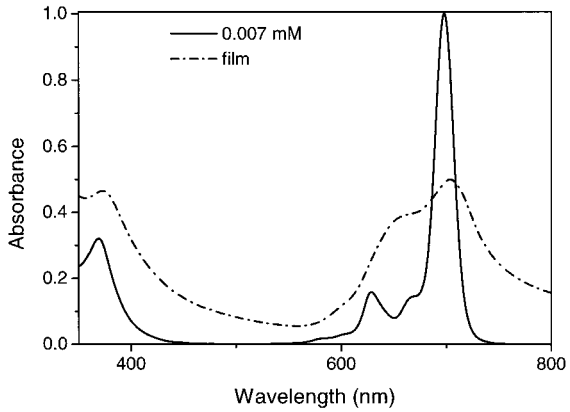

Figure 5. Absorption spectrum of a 7×10^{-6} M solution of (*t*-Bu)$_4$PcIn(*p*-TMP) in $CHCl_3$ compared to that of a thin film of the pure material.

band shape was a wing near 800 nm that appeared in the concentrated samples. This was most prominent in the concentrated (*t*-Bu)$_4$PcInCl sample and less so in the aryl-substituted compounds. Qualitatively, this is spectral evidence that the aggregation is less extensive in these axially substituted materials than in, for example, the tetrakis(cumylphenoxy)-substituted phthalocyanines. The latter showed much more pronounced spectral changes at over this range of concentrations.[37] Similarly, we conclude that the intermolecular interactions are weaker in the aryl-substituted compounds compared with the chloro compound.

We also recorded spectra of pure thin films of these materials. Figure 5 shows the spectrum of a pure film of (*t*-Bu)$_4$PcIn(*p*-TMP) and, for comparison, the spectrum of an approximately 7×10^{-6} M solution. Similar absorbance spectra have been observed in concentrated[38] polymeric thin films of (*t*-Bu)$_4$PcInCl. The absorption spectrum of the thin film is broader, as expected, and includes a wing beyond 800 nm, but the position of the Q-band is only slightly shifted between the thin film and the dilute solution. This is consistent with relatively weak aggregation in these axially substituted In phthalocyanines.

Nonlinear Optical Experiments. Our objective here is to quantify the nonlinear optical response in these materials and to determine how it varies with axial substitution. For practical optical limiters, the nonlinear absorption and refraction on the time scale of a few nanoseconds are of most interest. They will

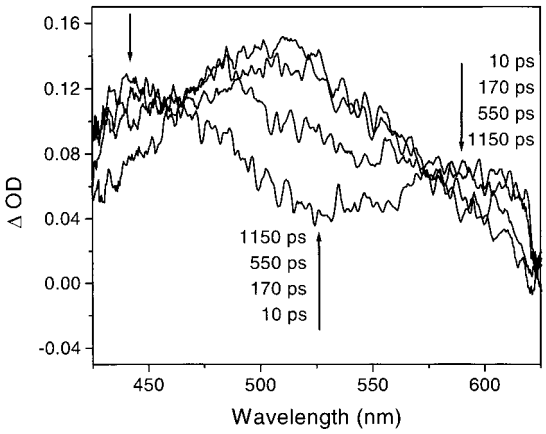

Figure 6. Evolution of the change in the absorption spectrum (ΔOD) of 5 mM solution of (*t*-Bu)$_4$PcInCl in $CHCl_3$ at different times after excitation at 725.5 nm.

be the emphasis here. We use nonlinear absorption and Z-scan measurements to determine the absorptive and refractive components of the nonlinear optical response and its wavelength dependence. Nanosecond nonlinear transmission measurements give the effective excited state cross sections and nonlinear absorption coefficients. When carried to very high fluences, they also enable us to study higher order nonlinear processes important to practical optical limiters.

In our lab, the initial studies of a new material are normally time-resolved studies of the dynamics of the materials. Here we report picosecond DFWM and transient absorption measurements that yield the excited state cross sections, lifetimes, and the intersystem crossing rates. These experiments establish whether the materials possess the cross sections and lifetimes that are the prerequisites of any useful optical limiter material.

Time-Resolved Measurements. This section concentrates on measurements of the dynamics of the nonlinearities in these materials. The main interest is in clarifying the mechanisms that lead to the observed nanosecond nonlinearities. Transient absorption spectra give the wavelength dependence of the pertinent excited state absorptions and the dynamics of the evolution of the excited states. DFWM measurements also give a measure of the excited state dynamics and the orientational relaxation times of the molecules in solution. In order to determine how the nonlinearities evolve, the dynamics are measured on the picosecond time scale.

Transient absorption studies of the chloro compound (*t*-Bu)$_4$PcInCl are shown in Figure 6. This shows the change in the absorption spectrum after excitation directly into the Q-band with a 1.2 ps (fwhm) pulse at 725.5 nm. The spectra recorded at 10 ps, 170 ps, 550 ps, and 1.15 ns after excitation are shown. These were selected from a more extensive series of spectra at different delay times. The spectrum at 10 ps shows an increase in the absorbance, i.e., a positive ΔOD, over the wavelength range between 420 and about 620 nm. The upper state cross section of the initially excited singlet state is greater than that of the ground state over this wavelength range. There were peaks in the difference spectra near 440 nm and near 600 nm.

The initial spectrum evolves into a spectrum peaked at 510 ± 10 nm. The approximate isosbestic points near 460 and 590 nm are consistent with the presence of only two excited states, one of which evolves into the other. It is consistent with an initially excited singlet state, the carrier of the 10 ps spectrum, evolving with a quantum yield near 1 to a triplet state, the carrier of the 1.15 ns spectrum. The intersystem crossing time estimated from a series of transient absorption studies was approximately 300 ps. With this relatively fast intersystem crossing rate, the

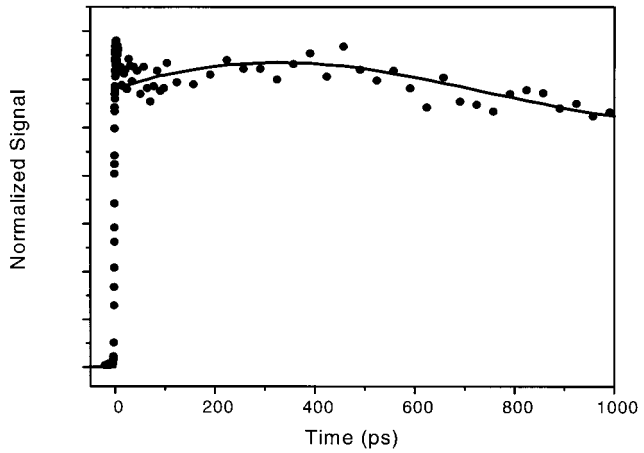

Figure 7. Degenerate four-wave mixing signal at 590 nm (*xxxx* polarization) of a 7.7 mM solution of (*t*-Bu)$_4$PcInCl in $CHCl_3$ as a function of the time delay.

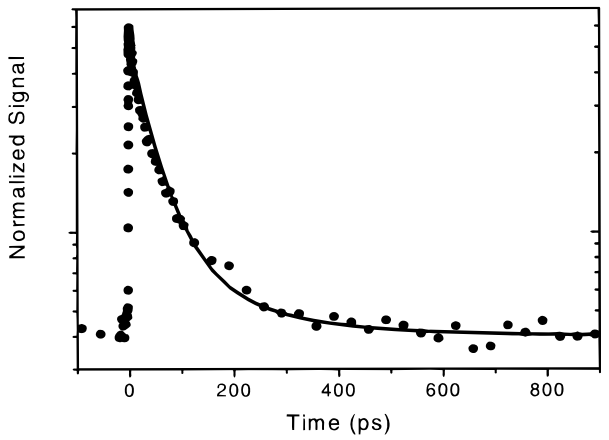

Figure 8. Degenerate four-wave mixing signal at 590 nm (*xyyx* polarization) of a 7.7 mM solution of (*t*-Bu)$_4$PcInCl in $CHCl_3$ as a function of the time delay.

triplet absorption spectrum will dominate the nanosecond nonlinear response.

We also performed DFWM experiments using a phase conjugate geometry. Figure 7 shows the DFWM signal at 590 nm from (*t*-Bu)$_4$PcInCl using all copolarized beams, the *xxxx* polarization. In this figure, the time dependence was determined by delaying the back pump beam. Except for the coherent peak when all three beams interact in the sample, a signal appears in less than 10 ps and then evolves slowly compared with the laser pulse width. This is expected when the nonlinear response is dominated by optical pumping of an excited state.[39] Thus, we conclude that the observed DFWM signal is due to an excited state grating.

It is possible to draw some qualitative conclusions about the nature of the nonlinearities involved from Figure 7.[40] The grating efficiency, η, of an excited state grating is[41]

$$\eta \propto (\Delta\alpha)^2 + (\Delta n_{ex} + \Delta n_{acoustic})^2$$

where $\Delta\alpha$ is the modulation in the sample absorbance, Δn_{ex} is the modulation in the refractive index due to the excited state, and $\Delta n_{acoustic}$ is the modulation in the index due to the acoustic grating generated from the deposition of heat at the grating maxima. The line in Figure 7 is the time dependence of the DFWM signal expected from the excited state evolution found in the transient absorption experiment (Figure 6) and an acoustic signal with a period of 2.5 ns. The latter is determined from the pumping geometry. The rise in the signal with a 300 ± 30 ps lifetime in Figure 7 is identified with the intersystem crossing rate. Since we know from the transient absorption experiment that the $\Delta\alpha$ is small at this wavelength, the DFWM signal is due primarily to a refractive index grating. We can then compare the signs of the acoustic and excited state contributions to the index changes. Qualitatively in Figure 7, the acoustic signal, most apparent at times longer than 600 ps, subtracts from the excited state contribution. Thus, the index change of the acoustic signal is of the opposite sign from the index change from the formation of the triplet state. Since $\Delta n_{acoustic}$ must be negative, we conclude that Δn_{ex} is positive. Further, since the intersystem crossing from the singlet state to the triplet state causes an increase in the DFWM signal, the refractive index of the triplet state at 590 nm must be larger than that of the singlet state. This information is useful for assessing the refractive contributions to optical limiting.

We confirmed the contribution of the acoustic signal in another experiment using the all-parallel-polarized configuration (*xxxx*). In our apparatus, delaying the front pump beam gives a larger angle between the beams that create the grating. Thus, the grating spacing is smaller and the acoustic period is shorter. In this case, the DFWM signal was analogous to that in Figure 7, except that the period of the acoustic signal was 206 ps, in agreement with the calculated period for the more closely spaced grating.

In the all-parallel-polarized DFWM experiment, the excited state is formed with orientational order. In principle, the decay of this order can contribute to the decay of the DFWM signal. To investigate this, the orientational decay time was found from a DFWM experiment with cross polarized beams.[42] Figure 8 shows the time dependence of the DFWM signal from (*t*-Bu)$_4$PcInCl with crossed polarized beams, the *xyyx* polarization. The best fit to an exponential decay for this signal gives an orientational correlation time of 170 ps. This is reasonable for the rotational time of an indium phthalocyanine with *tert*-butyl substituents on the periphery.[43] The ratio of the *xyyx*/*xxxx* signal was near 0.014. This is smaller than the usual ratio of $^1/_9 = 0.11$ expected for a nondegenerate transition[39,41] because the excited state arising from excitation into the Q-band is either degenerate or near degenerate in these molecules. Excitation of a 2-fold degenerate state gives a smaller absorption anisotropy[44] and a correspondingly smaller *xyyx* signal. Since the orientational correlation time is 170 ps and there is only a small orientational anisotropy, the nanosecond nonlinear absorption will be dominated by absorption from an orientationally averaged excited state population.

We performed DFWM measurements on each of the In phthalocyanines described here. The intersystem crossing rates were all within experimental error of 300 ps, and the triplet state lifetimes were all much longer than 5 ns. The orientational correlation time was slightly longer, 200 ± 30 ps, in (*t*-Bu)$_4$PcIn(*p*-TMP) than in the chloro compound.

To summarize the results of the picosecond experiments: excitation into the Q-band gives an initially excited singlet state that evolves into a triplet state with a quantum yield near 1 and an intersystem crossing rate of 300 ± 30 ps. The lifetime of this triplet state is long compared to 5 ns. In both the triplet and singlet state, the excited state cross section is larger than that of the ground state over the range between 420 and about 620 nm. The refractive index of both excited states is larger than that of the ground state at 590 nm so that the change in refractive index upon excitation is positive. The orientational correlation time is about 170 ps. Thus, the nanosecond optical

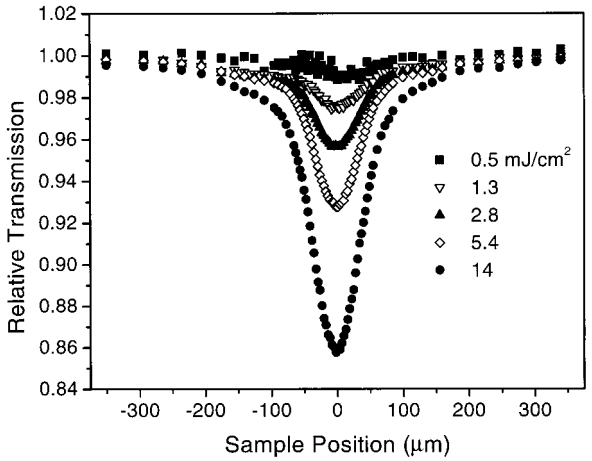

Figure 9. Relative transmission at 532 nm of a 45 mM solution of (*t*-Bu)$_4$PcIn(*p*-TMP) in $CHCl_3$ as a function of the distance from the focus (open aperture Z-scan). The peak on axis fluence at the focus is given for each scan.

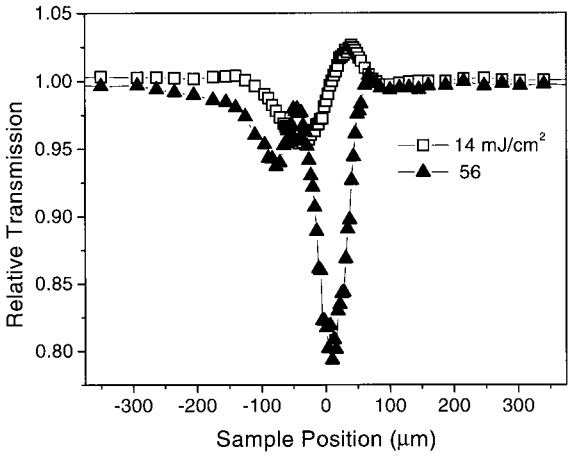

Figure 10. Relative transmission through a 40% aperture at 532 nm of a 45 mM solution of (*t*-Bu)$_4$PcIn(*p*-TMP) as a function of sample position divided by the open aperture Z scan. The peak on axis fluence at the focus is given for each scan.

limiting in this material will be dominated by the absorption from an orientationally averaged triplet state.

Nanosecond Z-Scan Measurements. We performed nanosecond Z-scan measurements on each of these materials with the apparatus shown in Figure 2 using *f*/5 optics. We measured the sample transmission at 532 nm as a function of sample position along the optical axis, first with an open exit aperture (A2 in Figure 2) and then with an exit aperture set to give a 40% transmission when the sample was far from the focus. The transmission was recorded using peak fluences from 0.2 to 60 mJ/cm^2 at the focus.

The open aperture Z-scan for a 45 mM solution of (*t*-Bu)$_4$PcIn(*p*-TMP) in $CHCl_3$ nm is shown in Figure 9. This shows that the material has a positive nonlinear absorption constant; i.e., it is a reverse saturable absorber over this range of fluences. The nonlinear absorption coefficient was within experimental error of that determined from the nonlinear transmission data described below.

Figure 10 shows the transmission with the 40% aperture as a function of sample position at two different fluences. The data has been divided by the open aperture transmission at each point. This procedure yields the effect of nonlinear refraction only[45] so long as the two contributions are separable. In Figure 10, the scan at 14 mJ/cm^2 shows a shape characteristic of a sample with a positive nonlinear index of refraction. This is consistent with an increase in index of refraction upon excitation to the triplet state. At higher fluences, the shapes of these refractive Z-scans become more complex. There appears to be a process with a negative change in the index superimposed on the lower fluence scan. We attribute the latter to a contribution from a thermal change in the index of refraction. Since the solution expands on heating, the thermal change in the index is negative. This thermal contribution does not simply add to the electronic one, because with *f*/5 optics and nanosecond pulses, the thermal nonlinearity is in the transient regime.[46] This means the thermal expansion does not reach an equilibrium across the beam diameter during the laser pulse. In contrast, the excited state population is always proportional to the local fluence in the beam. In Figure 10, when the sample is well away from focus ($z \sim -200\ \mu$m), the thermal change in the index does not have sufficient time to propagate across the relatively large beam diameter, so the refractive nonlinearity is mainly due to the excited state. When the sample is near the focus ($z \sim 0$), the beam diameter is small enough so that at high enough fluences, the thermal expansion can contribute to and even dominate the refractive index changes. The data in Figure 10 at 56 mJ/cm^2 shows evidence for both contributions as the sample position varies. The thermal contribution to the nonlinear refraction is negative and the excited state contribution is positive.

These Z-scan experiments are consistent with the results from the DFWM measurements. In the latter, the two contributions to the refractive nonlinearity are of opposite signs at 590 nm. The different contributions to the nonlinear refraction will tend to cancel. They give the refractive index in these samples a complicated time and spatial dependence. At high fluences, where refractive effects contribute to optical limiting, the dominant contribution is the thermal one for which there is a negative change in the index of refraction.

The Z-scans of the other two In phthalocyanines were like that observed in (*t*-Bu)$_4$PcIn(*p*-TMP). In each case there was a large positive nonlinear absorption and both a thermal and an excited state nonlinear refraction. The nonlinear absorption coefficients of these materials were consistent with those found from the nonlinear transmission data below. The magnitudes of the nonlinear refraction coefficients can be determined from the Z-scan data. However, in this case, modeling the combined thermal and excited state refractive response to obtain the nonlinear refractive contributions quantitatively is beyond the scope of this paper.

Nanosecond Nonlinear Transmission. The transmission as a function of incident fluence was measured for samples of each of the In phthalocyanines over a range of wavelengths between 500 and 620 nm. The results for selected sets of these measurements are shown in Figure 11. In this experiment the input optics were approximately *f*/45 and the collection aperture was approximately *f*/5. The sample was positioned at the focus of the laser. Under these conditions, there is little contribution from refractive nonlinearities so that the data represents nonlinear absorption only.

The nonlinear transmission for (*t*-Bu)$_4$PcInCl at several wavelengths is shown in Figure 11a. In this figure the initial change in transmission, corresponding to the onset of nonlinear absorption and optical limiting, occurs at smaller incident fluences as the wavelength increases from 500 to 570 nm. The threshold for optical limiting was defined as the fluence at which the transmission falls to 0.5 of the initial transmission. It is seen that the threshold varies by about an order of magnitude over this range of wavelengths. At 590 nm the value of the ground

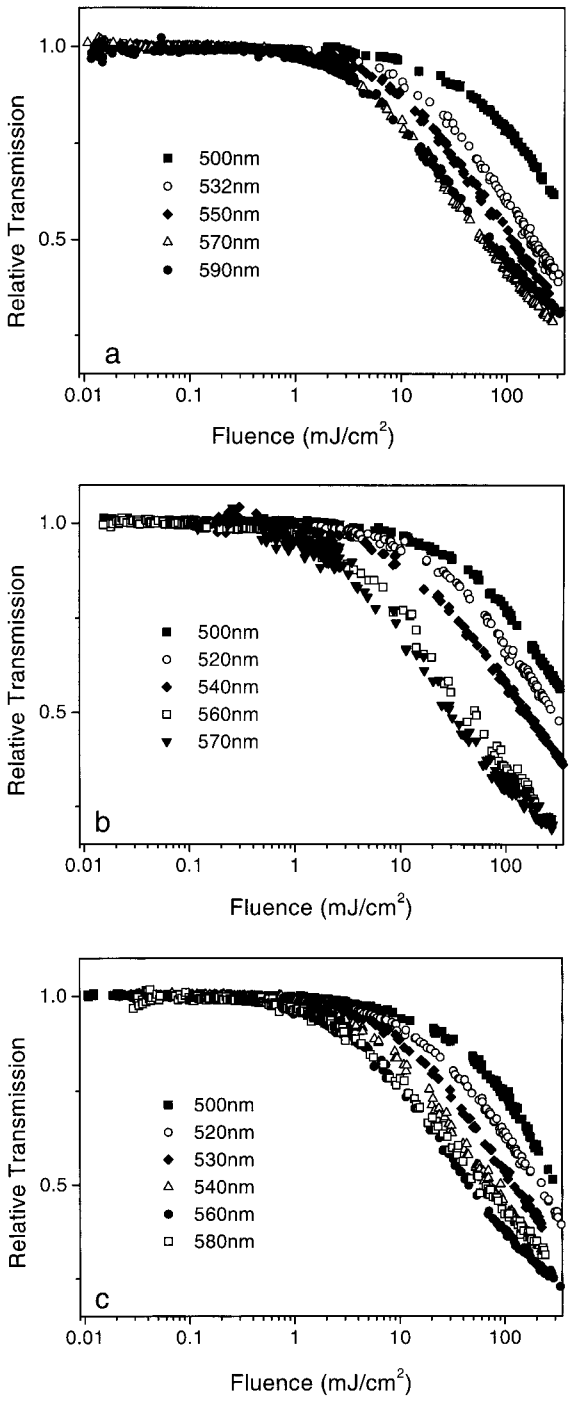

Figure 11. Normalized transmission of (a, top) (*t*-Bu)$_4$PcInCl, (b, middle) (*t*-Bu)$_4$PcIn(*p*-TMP), and (c, bottom) (*t*-Bu)$_4$PcInPFP as a function of incident fluence at different wavelengths. Each material was a 7.0 mM solution in $CHCl_3$.

state absorption cross section, σ_0, is approaching that of the excited triplet state, σ_T. Nonetheless, the limiting threshold at 590 nm is lower than at 500 nm where the value of the ratio σ_T/σ_0 is greater than 30. At 590 nm the nonlinear absorption shows evidence of saturation between 100 and 200 mJ/cm^2.

Figure 11, b and c, shows the variation of the transmission with the fluence for the two aryl-substituted In phthalocyanines. In both of the aryl-substituted materials the nonlinear absorption begins at a lower fluence than for (*t*-Bu)$_4$PcInCl. In addition, the aryl-substituted materials show a stronger nonlinear absorption and the threshold improves with increasing wavelength.

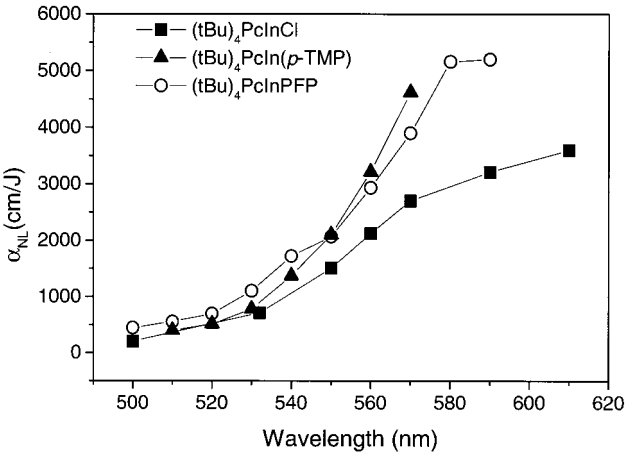

Figure 12. Measured nonlinear absorption coefficients of 7.0 mM solutions of (*t*-Bu)$_4$PcInCl, (*t*-Bu)$_4$PcIn(*p*-TMP), and (*t*-Bu)$_4$PcInPFP as a function of wavelength.

For these excited state absorbers, the initial change in transmission can be expressed as a fluence-dependent absorption,[5] $\alpha(F)$, that varies with a nonlinear absorption coefficient, α_{NL}, that can be defined so that

$$\alpha(F) = \alpha_0 + \alpha_{NL}F$$

where $\alpha(F)$ is the observed absorption coefficient as a function of the incident fluence, F, and α_0 is the linear absorption coefficient at low intensity. The nonlinear absorption coefficient, α_{NL}, is proportional to the initial slope of the transmission vs fluence graphs in Figure 11. The nonlinear absorption coefficient, $\alpha_{NL}(F)$, can be determined[5] from

$$\alpha_{NL} = S/L_{eff}$$

where S is the slope determined from a least-squares fit of a plot of the inverse of the transmission vs the fluence and L_{eff} is the effective path length of the sample.

$$L_{eff} = \frac{1 - e^{-\alpha_0 L}}{\alpha_0}$$

The measured nonlinear absorption coefficient as a function of wavelength is shown in Figure 12 for each of the subject compounds. These coefficients are derived from the nonlinear transmission data.

The fluence-dependent nonlinear absorption coefficient increases with wavelength between 500 and 570 nm for each material. The aryl-substituted phthalocyanines have nonlinear absorption coefficients that are generally larger than those of the chloro compound over most of this wavelength range.

Optical Limiting. Practical optical limiters will probably first be used in systems that have efficient light collection and a wide field of view. This means optical systems characterized by small *f*/numbers. The tight focus and small depth of field found in such systems put constraints on the properties of the nonlinear material. In the optical limiting experiments, we characterize the transmission as a function of input energy using *f*/5 optics and an input beam that has a flat spatial profile to simulate light from a distant source. The rationale is to examine the nonlinear optical properties under conditions where the materials might be used.

Figure 13 shows the limiting for a 30 mM solution of (*t*-Bu)$_4$PcInCl with a path length of 32 μm. This figure gives the transmitted energy as a function of input energy at 532 nm.

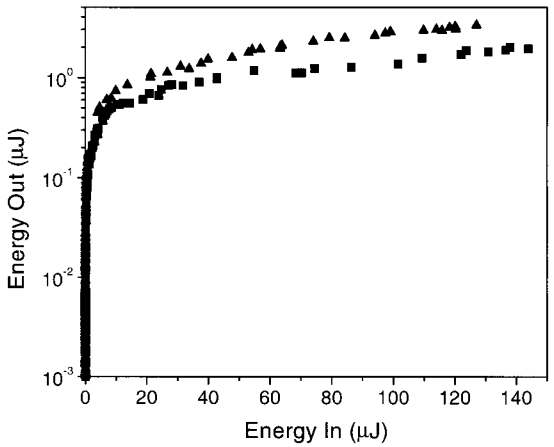

Figure 13. Optical limiting at 532 nm by a 30 mM solution of (*t*-Bu)$_4$PcInCl. The phthalocyanine solution transmission was 0.88 and the total sample transmission, including window losses, was 0.81. The lower curve (squares) is the transmission of an *f*/5 optical limiter. The upper curve (triangles) is the transmitted energy with an open exit aperture to give *f*/0.8 collection optics.

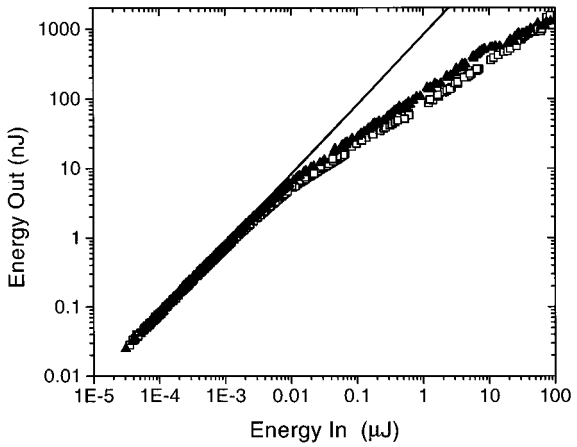

Figure 14. Incident vs transmitted energy for an *f*/5 optical limiter at 532 nm. The limiter materials were a 30 mM solution of (*t*-Bu)$_4$PcInCl (upper curve, triangles) and a 45 mM solution of (*t*-Bu)$_4$PcIn(*p*-TMP). (lower curve, squares). The concentrations were chosen to give the same initial transmission at 532 nm.

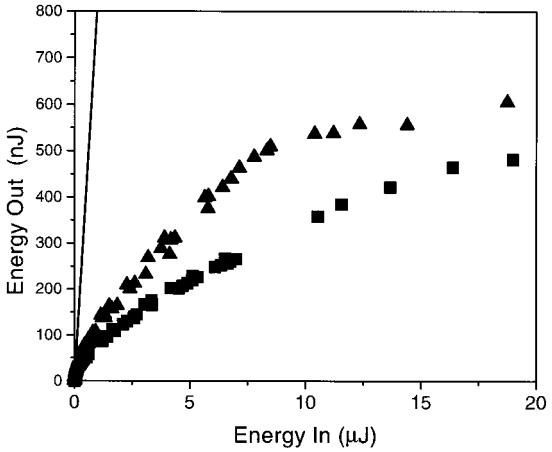

Figure 15. Incident vs transmitted energy for an *f*/5 optical limiter at 532 nm using a 30 mM solution of (*t*-Bu)$_4$PcInCl (upper curve, triangles) and a 45 mM solution of (*t*-Bu)$_4$PcIn(*p*-TMP) (lower curve, squares). The scale was chosen to show the limiting when the transmitted energy is in the range of a few hundred nanojoules.

The input optics were *f*/5. The low-intensity transmission of the sample was measured independently to be 0.81, comprising a phthalocyanine solution transmission of 0.88 and a cell transmission of approximately 0.92. The cell losses were due to reflection at the windows. The sample was positioned near the focus to give the minimum transmitted energy near the limiting threshold. In the upper curve (triangles), the transmitted energy is collected with an *f*/0.8 lens, so that the curve represents primarily the losses due to nonlinear absorption alone. The lower curve (squares) is the transmitted energy with an *f*/5 aperture at the exit plane. At low input intensities, this aperture transmits all the incident light. At high fluences, nonlinear refraction effects cause the sample to behave as a lens with strong aberrations. This aberrated lens causes some of the transmitted light to be deflected into the wings of the transmitted beam, where it is blocked by the exit aperture. This is the nonlinear refraction effect previously identified in the Z-scan measurements. The difference between the *f*/0.8 and *f*/5 collection is a measure of the contribution of nonlinear refraction to the limiting. An optical limiter device will follow the lower curve with contributions from both nonlinear absorption and refraction. The beam aberrations contribute substantially to the observed optical limiting. At input energies above about 30 μJ, the transmission of the *f*/5 limiter is about a factor of 2 lower than that due to nonlinear absorption alone.

The limiting using one of the aryl-substituted materials is shown in Figure 14. This figure shows a comparison of (*t*-Bu)$_4$PcInCl in the upper curve (triangles), and (*t*-Bu)$_4$PcIn(*p*-TMP) in the lower curve (squares). The (*t*-Bu)$_4$PcIn(*p*-TMP) sample had a concentration of 45 mM and was in a cell with a path length of 32 μm. The higher concentration was chosen to make the initial transmission of the two samples approximately equal at $T_0 = 0.81$. Again, this includes a cell transmission of 0.92, due to reflection at the windows, and a phthalocyanine transmission of approximately 0.88. This graph is on a log−log scale, a view that illustrates the wide range over which limiting occurs in both these materials. The *p*-TMP-substituted material had a threshold, the input energy at which $T/T_0 = 0.5$, of 19 ± 3 nJ whereas the Cl-substituted material had a threshold of 34 ± 4 nJ. The lower threshold for the (*t*-Bu)$_4$PcIn(*p*-TMP) material is consistent with the larger nonlinear absorption coefficient measured above. The *p*-TMP-substituted material had a lower transmission throughout the limiter range, although at very high fluences the transmission of the two materials began to converge. We also studied limiting by the (*t*-Bu)$_4$PcInPFP. The threshold at 532 nm was lower than for that for (*t*-Bu)$_4$PcInCl. However, this material was susceptible to photochemical degradation at input energies above 20 μJ, so we did not study it at the highest fluences.

The purpose of a limiter device is to limit the transmitted fluence to below some maximum value. Thus, in addition to the threshold and the high fluence transmission, another criterion for characterizing a limiter device is the maximum input energy before the output exceeds the desired maximum value. Figure 15 shows the same data as Figure 14, except that this graph is on a linear scale. If we take, as an example, the maximum permissible transmitted energy as 250 nJ,[47] this view clearly illustrates the differences in limiting between these materials in this range. The transmission of the *p*-TMP-substituted material is almost a factor of 2 lower than that of (*t*-Bu)$_4$PcInCl. Thus, (*t*-Bu)$_4$PcIn(*p*-TMP) can protect subsequent devices to nearly twice the input fluence compared to the chloro-substituted material.

Discussion

Time-Resolved Studies. As Figure 12 shows, each of these axially substituted indium phthalocyanines has a large, positive,

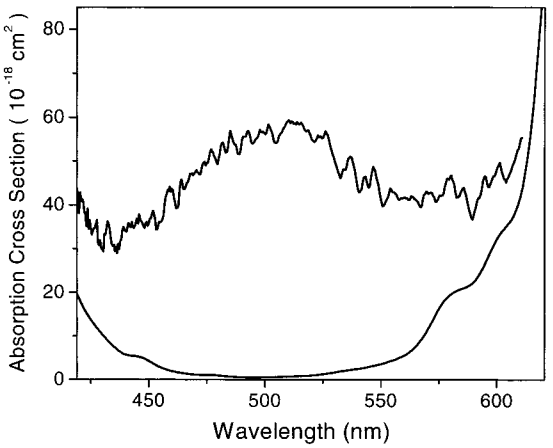

Figure 16. Ground and excited triplet state absorption spectra of (*t*-Bu)$_4$PcInCl.

TABLE 1: Properties of (*t*-Bu)$_4$PcInCl at 532 nm

	σ_g	σ_T	σ_T/σ_g	τ_{isc} (ps)
this work	1.8×10^{-18}	6.0×10^{-17}	33	300 ± 30
previous work[33,48]	1.6×10^{-18}		30	300 ± 30

nonlinear absorption coefficient across the visible. The mechanism for the nonlinear absorption is sequential two-photon absorption. The transient absorption experiments (Figure 6) show that both the initially formed singlet state and the triplet state have excited state absorption cross sections greater than that of the ground state, σ_0. The initial nonlinear response involves several processes and has a complex time dependence. However, the intersystem crossing and orientational relaxation had lifetimes of 200−300 ps. On a nanosecond time scale, the nonlinear absorption is dominated by the orientationally averaged lowest triplet state. Consequently, the simple energy level diagram shown in Figure 1, with the lowest triplet as the pertinent excited state, is a good approximation for the initiation of the limiting. The lifetime of this triplet excited state is much longer than 5 ns, so that for a typical pulsed laser with a pulse width of a few nanoseconds, the nonlinear absorption coefficient is fluence, rather than intensity, dependent.

The absorption cross sections of the triplet state of (*t*-Bu)$_4$PcInCl are shown in Figure 16. They were derived from the data in Figure 6 assuming that the triplet quantum yield is approximately 1. The triplet has a strong absorption across the visible, with a maximum near 515 nm. A positive nonlinear absorption is expected from less than 420 nm to about 600 nm.

The photophysical properties of the chloro indium phthalocyanine (*t*-Bu)$_4$PcInCl, were previously reported at 532 nm by Perry et al.[33,48] A comparison of the previously reported data with this work is in Table 1. The agreement is quite good.

Nanosecond Nonlinear Transmission. The fluence-dependent nonlinear absorption coefficients, α_{NL}, in Figure 12, increase substantially with increasing wavelength between 500 and 600 nm. The measured values of α_{NL} for the (*t*-Bu)$_4$PcInPFP material were larger than those for (*t*-Bu)$_4$PcInCl. Those for the *p*-TMP compound were similar to those for the Cl-substituted material near 500 nm, but larger at longer wavelengths. Consequently, both of the aryl-substituted materials will exhibit lower thresholds for optical limiting over this wavelength range.

The time-resolved data show that the nanosecond transmission is dominated by an orientationally averaged triplet state. We can then analyze the transmission data using the set of energy levels shown in Figure 1. Considering only the triplet excited state absorption, the equation describing the irradiance, *I*, as a function of the depth, ζ, of the sample is

$$-\frac{dI}{d\zeta} = \sigma_0 N_0 + N(\sigma_{ex} - \sigma_0) \quad (1)$$

where σ_0 is the ground state absorption cross section, σ_{ex} is the absorption cross section of the triplet excited state, and *N* and N_0 are the number density of the absorber in the excited and ground state, respectively. If the laser pulse is much shorter than the upper state relaxation time, then the rate of excited state production is

$$\frac{dN}{dt} = \frac{\sigma_0 N_0 I}{h\nu} \quad (2)$$

Following the discussion of Van Stryland et al.,[5] by integrating eq 2 from $t = 0$ to $t = t'$, substituting for *N* in eq 1, and integrating over all t', we get the dependence of the fluence, *F*, on the depth of the sample, ζ

$$-\frac{dF}{d\zeta} = (\alpha_0 + \alpha_{NL}F)F \quad (3)$$

where what is defined as the fluence-dependent nonlinear absorption coefficient, α_{NL}, with units of cm/J, is related to the absorption cross sections by

$$\alpha_{NL} = (\sigma_{ex} - \sigma_0)\frac{\sigma_0 N_0}{2h\nu} \quad (4)$$

In eq 4 the nonlinear absorption coefficient depends on the product, $\sigma_0(\sigma_{ex} - \sigma_0)$. Near 500 nm where $\sigma_{ex} \gg \sigma_0$, α_{NL} is expected to increase approximately linearly with σ_0. This can be seen in the experimental data by comparing the wavelength variation of the cross sections in Figure 4 with that of the α_{NL}'s in Figure 12.

The α_{NL}'s in Figure 12 are for 7.0 mM solutions. The differences in the α_{NL} between the materials are due to differences in $\sigma_0(\sigma_{ex} - \sigma_0)$. The larger α_{NL} for the *p*-TMP-substituted material compared to the Cl-substituted material is due to a larger excited state cross section between 500 and 600 nm. In the PFP-substituted material, both σ_{ex} and σ_0 are larger than those in the Cl compound across the measured wavelength range.

The σ_{ex}/σ_0 ratio is sometimes advocated as a figure of merit for excited state nonlinear absorbing materials.[48] However, in these indium phthalocyanine materials the nonlinear absorption *increases* substantially while the σ_{ex}/σ_0 ratio *decreases* from 33 to about 2. The cross section ratio does not characterize the strength of the nonlinear absorption. In fact, eq 4 shows that for a constant linear absorption, $\sigma_0 N$, the cross section difference, $\sigma_{ex} - \sigma_0$, is a more useful figure of merit.

We did compare the effective excited state cross section from the measured α_{NL}'s using eq 4 with those measured in the time-resolved transient absorption experiment. For (*t*-Bu)$_4$PcInCl, these effective nanosecond excited state cross sections were about 25% larger than the cross sections measured in the time-resolved transient absorption experiments in the range between 500 and 560 nm. The effect seems real, although the uncertainty in the σ_T derived from the nanosecond experiments is large where the ground state absorption coefficient is small. The difference in the measured σ_T's may arise from the different pump wavelengths used. In the picosecond time-resolved experiments, the sample was excited at 725.5 nm, on the red side of the Q-band. In the nanosecond nonlinear absorption experiments, the excitation was between 500 and 620 nm, at

the wavelength where the absorptions were measured. In the ground state absorption spectra, a weak aggregate absorption appears on the red side of the Q-band. Further work is necessary to decide if aggregation can account for the difference in apparent excited state cross section.

Optical Limiting. The threshold for an *f*/5 optical limiter was almost a factor of 2 lower at 532 nm in the aryl-substituted *p*-TMP phthalocyanine than in the chloro-substituted material. The reason can be traced to the larger nonlinear absorption coefficient, α_{NL}. In each material, the α_{NL} increases by almost an order of magnitude between 500 and 570 nm. The threshold for limiting will also improve with wavelength. The differences in threshold between the materials varied with wavelength, but the aryl-substituted materials always had a threshold that was equal to or smaller than the chloro compound. At some wavelengths, it was lower by almost a factor of 2 in the aryl-substituted materials.

In addition to possessing a low threshold, a practical limiter should also limit a large range of fluences. The low-intensity transmission of any absorber is

$$T_0 = e^{-\sigma_0 NL}$$

where N is the concentration of the absorber, L is the effective path length, and σ_0 is the ground state absorption cross section. In the four-level model using the energy levels of Figure 1, at high incident intensity, the ground state population is largely depleted[49] so the minimum possible high-intensity transmission is

$$T_H \approx e^{-\sigma_{ex} NL}$$

So in the four-level model the largest possible ratio of the transmissions is

$$\frac{T_0}{T_H} \approx e^{((\sigma_{ex}-\sigma_0)NL)}$$

This ratio of transmissions has been defined as a figure of merit for a limiter device.[50] It is maximized in a material for which the *difference* between the upper state and ground state absorption cross sections is a maximum. Again, using the ratio σ_{ex}/σ_0 as a figure of merit for the material in the device can be misleading. Experimentally, for these indium phthalocyanines, a $\sigma_{ex}/\sigma_0 \sim 10-20$ produces a reasonable threshold and the potential for a large reduction in transmission at high fluences. The σ_{ex}/σ_0 ratio of greater than 30 near 532 nm is a result of the small value of σ_0 at these wavelengths. This leads to the, perhaps counterintuitive, conclusion that the threshold could be improved in the region 500−540 nm if the materials could be modified to give an increase in σ_0.

The high fluence limiting was measured to incident energies of about a millijoule for the chloro- and the *p*-TMP-substituted material. The *p*-TMP-substituted material was a better limiter than the chloro-substituted material over the entire range of fluences. This material provides a lower transmission for a high input energy because of the larger excited state cross section. It may also be possible that the smaller degree of aggregation reduces deleterious intermolecular interactions in (*t*-Bu)$_4$PcIn(*p*-TMP).

Optical limiters based on (*t*-Bu)$_4$PcInCl have been previously reported by Perry et al.[33,48] Table 1 showed that the excited state cross sections and lifetimes reported in these studies are in good agreement with those reported here. The optical limiting results, however, do differ from those reported here because of different limiter designs. All of the limiter measurements used *f*/5 optics. The first of the limiters reported by Perry et al.[33] used a homogeneous solution of (*t*-Bu)$_4$PcInCl with a 1 cm path length and a low-intensity transmission of 0.70. The transmission of this limiter dropped to about 1.7% with about 8 mJ input energy. This group also describes an *f*/5 limiter that uses an inhomogeneous distribution of (*t*-Bu)$_4$PcInCl along the beam path.[33] In this "concentration gradient" limiter there is a larger fraction of the nonlinear absorber near the focus. The transmission of this limiter is about 1 order of magnitude lower than the first limiter at input energies well above threshold. In comparison, the (*t*-Bu)$_4$PcInCl limiter reported here had a higher initial transmission of 0.81 (of which 0.88 was due to the phthalocyanine solution)[51] yet it required only about 0.07 mJ of input energy before transmission dropped to about 1.7%. This is about 2 orders of magnitude less input energy to achieve the same limiting as the 1 cm path limiter and about 1 order of magnitude less than the concentration gradient limiter.

The more effective limiting described in this work is ascribed primarily to the shorter path length and higher concentration of the (*t*-Bu)$_4$PcInCl sample here. In the short path (32 μm) sample used in the present work, all of the nonlinear absorber is within the depth of focus of an *f*/5 limiter. In contrast, with a 1 cm path length, less than 0.5% of the (*t*-Bu)$_4$PcInCl is within the depth of focus. On the average, the sample is subjected to higher fluences in the short path length sample. The concentration gradient limiter is intermediate, and it has a larger concentration of phthalocyanine near the focus than the 1 cm cell, but less than the 32 μm cell. The observed transmission at fluences above the threshold is also intermediate.

The difference between these (*t*-Bu)$_4$PcInCl limiters is that the thin cell limiter described here has the lowest threshold and a lower transmission at high fluences. The advantage claimed for the concentration gradient limiter reported by Perry et al. is that the limiter *material* is protected from damage at high input fluences. Indeed they report limiting up to 8 mJ of input energy. The concentration gradient limiter may protect the limiter material from damage but at the cost of an increase in the total transmitted energy. The thin cell limiter reported here, where all the active material is within the focal volume, provides the lowest transmitted energy and the maximum protection of subsequent optical elements.

An additional contribution to the limiting in the thin cell limiter is nonlinear refraction. This can contribute significantly to the limiting, especially at higher energies. Recall that nonlinear refraction in the sample can cause a defocusing of the beam so that some of the light is removed by an aperture after the NLO material (A2 in Figure 2). The sample was positioned to take advantage of this effect. The contribution from nonlinear refraction in the limiter was measured by removing the output aperture and using an *f*/0.8 lens to collect essentially all the transmitted light. At energies well above the threshold, the transmitted energy using *f*/0.8 collection optics was approximately 2 times larger than with *f*/5 collection.

The properties of limiters based on nonlinear refractive effects have been discussed in some detail.[46,52,53] The limiting is most effective when the sample path length is less than the depth of focus. In these indium phthalocyanines, there are two sources of a refractive component to the limiting: a molecular n_2 derived from optical pumping of the excited state, and a thermal n_2 from the heating of the solvent by the absorbed energy. Both processes were found in each of these materials. Over the wavelength range examined, the sign of the n_2 is different for the two processes. It was recently reported that the nonlinear

refraction in a chloroaluminum phthalocyanine solution also shows two components with opposite signs.[54]

At fluences near the threshold, the total refractive contribution is not as large as might be expected since the two contributions tend to cancel each other. The low fluence limiting is primarily due to nonlinear absorption. However, for fluences well above the limiting threshold, the thermal contribution increases more rapidly than the excited state contribution when the sample is positioned near the focus. Experimentally, the thermal refractive contributions can make a substantial contribution to the high fluence limiting.

We found that in *f*/5 optical systems the spatial and temporal variations in the refractive index had a complex time dependence. There are now active efforts to perform numerical simulations of the beam propagation in optical limiters.[55,56] These refractive effects will need to be included for these simulations to accurately reflect the operation of a limiter using these materials.

Excited State Interactions. The high fluence limiting was measured to energies of about a millijoule. The nominal fluences in the sample range from several J/cm^2 to as much as 10^3 J/cm^2, depending on the sample position. The saturation fluence of these nonlinear materials is typically less than 1 J/cm^2. Since about 200 nJ into the entrance lens of an *f*/5 limiter produces fluences on the order of 1 J/cm^2 on a sample at the focus, the fractional population of the excited state is substantial over much of the range of interest to limiting. Thus, we would expect excited state−excited state interactions and multiphoton processes to contribute to the nonlinear absorption in this regime. The nature and rate of these excited state−exited state interactions are not completely understood, but they should depend the magnitude of the intermolecular couplings. They are likely to be sensitive to differences in concentration and especially sensitive to the size and structure of any molecular aggregates in the solution.

The high fluence absorbance will depend on the concentration of the excited state absorber in the beam. Thus, it is desirable to begin with a high concentration of the limiting material within the focal region of a limiter. However, as the concentration is increased, intermolecular interactions and aggregation will become more important. Among the photophysical processes that have been reported in aggregates, a shortened excited state lifetime is common.[57−59] A substantial shortening of the excited state lifetime is deleterious to a limiter because it will reduce the effective α_{NL} and increase the thresholds. It is desirable to design nonlinear materials that do not aggregate easily. These indium phthalocyanines seem to meet this criterion; they showed very little spectroscopic evidence for aggregation. Presumably the axial substituents inhibit aggregation. The only spectroscopic evidence for intermolecular interactions was a weak band on the long-wavelength side of the primary Q-band absorption in (*t*-Bu)$_4$PcInCl. In Figure 3, this aggregate band was even weaker in (*t*-Bu)$_4$PcIn(*p*-TMP) with a larger aryl substituent. The high fluence limiting was better in the latter material, although it is not clear if this is because there is the intermolecular interaction is reduced or because the σ_{ex} is larger.

Conclusions

The purpose of this work was to determine the optical properties of a series of indium phthalocyanines with aryl substituents at the axial position and to compare them with (*t*-Bu)$_4$PcInCl. The latter had been used previously to construct a good optical limiter. The emphasis was on the optical properties important to optical limiting of nanosecond pulses, specifically nanosecond nonlinear absorption and refraction.

In our original paper, 10 new aryl-substituted indium phthalocyanines were described.[34] We performed preliminary optical studies on most of these. We selected the materials with *tert*-butyl peripheral substitution for further studies because they were more soluble. Among the *tert*-butyl indium phthalocyanines, we chose the (*p*-trifluoromethyl)phenyl- and perfluorophenyl- axial substituents for detailed study. They showed promising optical properties, had evidence for little aggregation even at high concentrations, and provided a substantial difference in molecular structure compared with the chloro compound.

For each of these compounds, excitation into the visible gives an initially excited singlet state that evolves into a triplet state with a quantum yield near 1 and an intersystem crossing time of about 300 ps. The triplet state lifetime is long compared to 5 ns. The orientational correlation times were in the range 170−200 ps. Thus, in each of these compounds, the nanosecond nonlinear absorption is dominated by the absorption from an orientationally averaged triplet state. In both the triplet and singlet state, the excited state cross section is larger than that in the ground state over the range between 420 and about 620 nm. The refractive index of the triplet state is larger than that of the ground state at 532 and 590 nm, making the electronic contribution to the nonlinear refractive index positive. The thermal changes in index that appear in these materials are negative in sign. The interplay of these two contributions give the refractive index changes a complex time and spatial dependence. It will increase the difficulty of accurately modeling beam propagation in optical limiters using these materials.

The nonlinear absorption coefficients, α_{NL}, were measured between 500 and 620 nm. They were large and increased with increasing wavelength over the range 500−590 nm. The aryl-substituted materials had larger values of α_{NL} over much of this range. This larger α_{NL} resulted in lower thresholds for optical limiting in the aryl-substituted materials. The higher thresholds observed in the range 500 to about 530 nm were traced to a small ground state absorption cross section, σ_0. It was less than 2×10^{-18} cm^2 in this range.

In an *f*/5 limiter with a low-intensity transmission of 0.81 at 532 nm, the (*t*-Bu)$_4$PcIn(*p*-TMP) material had a lower threshold than (*t*-Bu)$_4$PcInCl, by about a factor of 2. At intermediate fluences, it can protect subsequent devices to nearly twice the input fluence compared to the chloro-substituted material. The (*t*-Bu)$_4$PcIn(*p*-TMP) showed a lower transmission than (*t*-Bu)$_4$PcInCl at all fluences above the threshold except at very high fluences where the difference between the materials decreased. The PFP-substituted material had a generally lower transmission than (*t*-Bu)$_4$PcInCl, but it was susceptible to photochemical degradation at high fluences. We conclude that the aryl-substituted indium phthalocyanine (*t*-Bu)$_4$PcIn(*p*-TMP) showed better transmission characteristics than the chloro compound.

Further improvements in the limiting by indium phthalocyanines could be realized by a small increase in the ground state cross section near the minimum absorbance. This would give a larger nonlinear absorption coefficient and a smaller threshold in this region. It could be achieved either by a change in molecular structure or by introducing a second absorber in this range, provided the absorber effectively transferred the excitation energy to the phthalocyanine. In addition, at low fluences, the refractive contributions to the limiting were small because the two contributions, electronic and thermal, have opposite signs. If the molecular structure could be altered to give a negative electronic contribution to the nonlinear refractive index, the limiting would be enhanced.

Perhaps the most remarkable result is that, among the materials studied here, the nonlinear optical properties of the In phthalocyanine moiety were quite robust to axial substitution. We found that a substantial variation in the axial substituent did not result in a loss of the characteristic large nonlinear absorption. In fact, a change in the axial substituent from chloro to the *p*-TMP substituent enhanced the optical limiting properties. This suggests that it may be possible to manipulate the molecular structure at the axial position to give the material desirable physical properties without large changes in the optical properties. For example, it might be feasible to incorporate an In phthalocyanine into a polymer backbone via the axial substituent to produce a nonlinear absorber at a very high concentration without degrading the nonlinear optical properties.

Acknowledgment. The work at NRL was supported by the Office of Naval Research. We also thank the Joint Services Agile Program and the NRL/ONR Laser Hardened Materials Project for support of the early part of this work. H.H. and M.H. thank the Fonds der Chemischen Industrie for support of part of the work.

References and Notes

(1) Nalwa, H. S.; Shirk J. S. In *Phthalocyanines: Properties and Applications;* Leznoff, C. C.; Lever, A. B. P., Eds.; VCH Publishers: New York, 1996; Vol. 4, p 79.

(2) Xia, T. J.; Hagan, D. J.; Dogariu, A.; Said, A. A.; Van Stryland, E. W. *Appl. Opt.* **1997**, *36*, 4110.

(3) Hermann, J. A.; Staromlynska, J. *Int. J. Nonlin. Opt. Phys*. **1993**, *2*, 271.

(4) Tutt, L. W.; Boggess T. F. *Prog. Quantum Electron.* **1993**, *17*, 299.

(5) Van Stryland, E. W.; Sheik-Bahae, M.; Said, A. A.; Hagan, D. J. *Prog. Cryst. Growth Charact.* **1993**, *27*, 279.

(6) Pittman, M.; Plaza, P.; Martin, M. M.; Meyer, Y. H. *Opt. Commun.* **1998**, *158*, 201.

(7) Chen, P. L.; Tomov, I. V.; Dvornikov, A. S.; Nakashima, M.; Roach, J. F.; Alabran, D. M.; Rentzepis, P. M. *J. Phys. Chem.* **1996**, *100*, 17507.

(8) de la Torre, G.; Vazquez, P.; Agullo-Lopez, F.; Torres, T. *J. Mater. Chem.* **1998**, *8*, 1671.

(9) Shirk, J. S.; Pong, R. G. S.; Bartoli, F. J.; Snow, A. W. *Appl. Phys. Lett*. **1993**, *63*, 1880.

(10) Coulter, D. R.; Miskowski, V. M.; Perry, J. W.; Wei, T.; Van Stryland, E. W.; Hagan, D. J. *SPIE Proc*. **1989**, *1105*, 42.

(11) Perry, J. W.; Khundkar, L. R.; Coulter, D. R.; Alvarez, D.; Marder, S. R.; Wei, T.; Sense, M. J.; Van Stryland, E. W.; Hagen, D. J. In *Organic Materials for Nonlinear Optics and Photonics*; Messier, J., Kajzar, F., Prasad, P. N., Eds.; NATO ASI Ser. E; Kluwer: Dordrecht, The Netherlands, 1991; Vol. 194, p 369.

(12) Wie, T. H.; Hagan, D. J.; Sence, M. J.; Van Stryland, E. W.; Perry, J. W.; Coulter, D. R. *Appl. Phys. B* **1992**, *54*, 46.

(13) Su, W.; Cooper, T. M. *Chem. Mater.* **1998**, *10*, 1212.

(14) Rao, D. N.; Rao, S. V.; Aranda, F. J.; Rao, D. V. G. L. N.; Nakashima, M.; Akkara J. A. *J. Opt. Soc. Am. B* **1997**, *14*, 2710.

(15) Wood, G. L.; Miller, M. J.; Mott, A. G. *Opt. Lett*. **1995**, *20*, 973.

(16) Tutt, L. W.; McCahon, S. W.; Klein, M. B. *SPIE Proc*. **1990**, *1307*, 315.

(17) McCahon, S. W.; Tutt, L. W.; Klein, M. B.; Valley, G. C. *SPIE Proc.* **1990**, *1307*, 304.

(18) Shang, X. M.; Zhang, G. L.; Liu, Y. Q.; Tang, G. Q.; Chen, W. J. *J. Phys. Chem. A* **1998**, *102*, 7487.

(19) Shi, S.; Hou, H. W.; Xin, X. Q. *J. Phys. Chem.* **1995**, *99*, 4050.

(20) Ji, W.; Shi, S.; Du, H. J. *J. Phys. Chem*. **1995**, *99*, 17297.

(21) Xia, T.; Dogariu, A.; Mansour, K.; Hagan, D. J.; Said, A. A.; Van Stryland, E. W.; Shi, S. *J. Opt. Soc. Am. B* **1998**, *15*, 1497.

(22) Smilowitz, L.; McBranch, D.; Klimov, V.; Robinson, J. M.; Koskelo, A.; Grigorova, M.; Mattes, B. R.; Wang R. C. H.; Wudl, F. *Opt. Lett.* **1996**, *21*, 922.

(23) Kost, A.; Jensen, J. E.; Klein, M. B.; McCahon, S. W. *SPIE Proc.* **1994**, *2229*, 78.

(24) Hoffman, R. C.; Stetyick, K. A.; Potember, R. S.; McLean, D. G. *J. Opt. Soc. Am. B* **1989**, *6*, 772.

(25) Healy, W.; Bahra, G. S.; Brown, C. R. *SPIE Proc*. **1994**, *2229*, 100.

(26) Hughes, S.; Spruce, G.; Wherrett, B. S.; Welford, K. R.; Lloyd, A. D. *Opt. Commun*. **1993**, *100*, 113.

(27) Hochbaum, A.; Hsu, Y. Y.; Fergason, J. L. *SPIE Proc*. **1994**, *2229*, 48.

(28) Justus, B. L.; Kafafi, Z. H.; Huston, A. L. *Opt. Lett.* **1993**, *18*, 1603.

(29) Kost, A.; Tutt, L.; Klein, M. B.; Dougherty, T. K.; Elias, W. E. *Opt. Lett.* **1993**, *18*, 334.

(30) Tutt, L. W.; Kost, A. *Nature* **1992**, *356*, 225.

(31) Hood, P J.; Edmonds, B. P.; McLean, D. G.; Brandelik, D. M. *SPIE Proc*. **1994**, *2229*, 91.

(32) Shirk, J. S.; Pong, R. G. S.; Flom, S. R.; Bartoli, F. J.; Boyle, M. E.; Snow, A. W. *Pure Appl. Opt*. **1996**, *5*, 701.

(33) Perry, J. W.; Mansour, K.; Lee, I. Y. S.; Wu, X. L.; Bedworth, P. V.; Chen, C. T.; Ng, D.; Marder, S. R.; Miles, P.; Wada, T.; Tian, M.; Sasabe, H. *Science* **1996**, *273*, 1533.

(34) Hanack, M.; Heckmann, H. *Eur. J. Inorg. Chem*. **1998**, 367.

(35) Shirk, J. S.; Lindle, J. R.; Bartoli, F. J.; Boyle, M. E. *J. Phys. Chem*. **1992**, *96*, 5847.

(36) Flom, S. R.; Pong, R. G. S.; Bartoli, F. J.; Kafafi, Z. H. *Phys. Rev. B* **1992**, *46*, 15598.

(37) George, R. D.; Snow, A. W.; Shirk, J. S.; Barger, W. R. *J. Porphyrins Phthalocyanines* **1998**, *2*, 1.

(38) Cumpston, B. H.; Mansour, K.; Heikal, A. A.; Perry, J. W. *Mater. Res. Soc. Symp. Proc*. **1997**, *479*, 89.

(39) Eichler, H. J.; Günter, P.; Pohl, D. W. *Laser Induced Dynamic Gratings*; Springer-Verlag: Berlin, 1986.

(40) Deeg, F. W.; Fayer, M. D. *J. Chem. Phys*. **1989**, *91*, 2269.

(41) Fayer, M. D. *IEEE J. Quantum Electron.* **1986**, *QE-22*, 1437.

(42) Meyers, A. B.; Hochstrasser, R. M. *IEEE J. Quantum Electron*. **1986**, *QE-22*, 1482.

(43) See examples in: Fleming, Graham, R. *Chemical Applications Of Ultrafast Spectroscopy*; Oxford University Press: New York, 1986.

(44) Naqvi, K. R.; Knox, R. S. *Phys. Rev. A* **1998**, *58*, 3360; Pfeffer, N.; Isoshima, T.; Tian, M. Q.; Wada, T.; Nunzi, J.-M.; Sasabe, H. *Phys. Rev. A* **1997**, *55*, R2507.

(45) Sheik-Bahae, M.; Said, A. A.; Wei, T. H.; Van Stryland, E. W. *IEEE J. Quantum Electron.* **1990**, *QE-26*, 760.

(46) Brochard, P.; Grolier-Mazza, V.; Cabanel, R. *J. Opt. Soc. Am. B* **1997**, *14*, 405.

(47) This limit was chosen as a measure of the maximum permitted fluence into an eye. The ANSI standard is currently of 0.5 μJ/cm^2, which, over an 8 mm diameter iris, corresponds to a maximum permitted energy of about 250 nJ.

(48) Perry, J. W.; Mansour, K.; Marder, S. R.; Perry, K. J.; Alvarez, D.; Choong, I. *Opt. Lett.* **1994**, *19*, 625.

(49) The maximum excited state fractional population will be limited by other excited state relaxation processes. In a real limiter it is unlikely that all the population could be transferred to an excited state.

(50) Hagan, D. J.; Xia, T.; Said, A. A.; Wei, T. H.; Van Stryland, E. W. *Int. J. Nonlin. Opt. Phys.* **1993**, *2*, 483.

(51) The phthalocyanine transmission of 0.88 is apparently the "internal transmission" reported in ref 33. Reflections at the cell windows account for the additional loss.

(52) Swartzlander, G. A., Jr.; Justus, B. L.; Huston, A. L.; Campillo, A. J.; Law, C. T. *Int. J. Nonlin. Opt. Phys.* **1993**, *2*, 577.

(53) Justus, B. L.; Huston, A. L.; Campillo, A. J. *Appl. Phys. Lett*. **1993**, *63*, 1483.

(54) Wei, T. H.; Huang, T.-H. *Appl. Phys. Lett.* **1998**, *72*, 2505.

(55) Kovsh, D.; Yang, S.; Hagan, D. J.; Van Stryland, E. W. *Proc. SPIE* **1998**, 3742, 163.

(56) Swartzlander, G. A.; Law, C. T. provide beam propagation program at the web site: superb.ind.wpi.edu/BeamProp/.

(57) Dhami, S.; Phillips, D. *J. Photochem. Photobiol. A* **1996**, *100*, 77.

(58) Flom, S. R.; Shirk, J. S.; Lindle, J. R.; Bartoli, F. J.; Kafafi, Z. H.; Pong, R. G. S.; Snow, A. W. *Proc. Mater. Res. Soc*. **1992**, *247*, 271.

(59) Oddos-Marcel, L.; Madeore, F.; Bock, A.; Neher, D.; Ferencz, A.; Rengel, H.; Wegner, G.; Kryschi, C.; Trommsdorff, H. P. *J. Phys. Chem*. **1996**, *100*, 11850.